



**University of  
Zurich**<sup>UZH</sup>

**Zurich Open Repository and  
Archive**

University of Zurich  
University Library  
Strickhofstrasse 39  
CH-8057 Zurich  
[www.zora.uzh.ch](http://www.zora.uzh.ch)

---

Year: 2012

---

## **Histopathological patterns of nephrocalcinosis: a phosphate type can be distinguished from a calcium type**

Wiech, T ; Hopfer, H ; Gaspert, A ; Banyai-Falger, S ; Hausberg, M ; Schröder, J ; Werner, M ;  
Mihatsch, M J

**Abstract:** **BACKGROUND:** The etiology of nephrocalcinosis is variable. In this study, we wanted to elucidate whether the histopathological appearance of calcium phosphate deposits provides information about possible etiology. **METHODS:** Autopsy cases from the years 1988 to 2007 and native kidney biopsies from a 50-year period (1959-2008) with nephrocalcinosis were identified. The biopsy cases were re-evaluated by light microscopy. The autopsy cases were analysed according to the underlying disease. The biopsy cases were grouped with respect to the likely etiology of nephrocalcinosis. Total number, density, localization, size and pattern of all calcification foci were documented and correlated with clinical and laboratory data. **RESULTS:** About 223 of 12 960 autopsy cases (1.7%) had nephrocalcinosis, 111 of which (49.8%) suffered from advanced malignant tumours. Nephrocalcinosis was the main diagnosis in 48 of 12 480 native kidney biopsies (0.4%). Clinicopathological correlation revealed a specific pattern of calcification associated with hyperphosphataemia and/or hyperphosphaturia: these cases showed predominant globular or shell-like calcifications (phosphate type). In contrast, the biopsies of the hypercalcaemic/hypercalciuric group had a different predominant pattern with clumpy or finely granular calcifications (calcium type). **CONCLUSIONS:** Our results indicate that hyperphosphaturia-associated cases of nephrocalcinosis can be distinguished from hypercalciuria-associated cases histopathologically.

DOI: <https://doi.org/10.1093/ndt/gfr414>

Posted at the Zurich Open Repository and Archive, University of Zurich

ZORA URL: <https://doi.org/10.5167/uzh-50420>

Journal Article

Published Version

Originally published at:

Wiech, T; Hopfer, H; Gaspert, A; Banyai-Falger, S; Hausberg, M; Schröder, J; Werner, M; Mihatsch, M J (2012). Histopathological patterns of nephrocalcinosis: a phosphate type can be distinguished from a calcium type. *Nephrology, Dialysis, Transplantation*, 27(3):1122-1131.

DOI: <https://doi.org/10.1093/ndt/gfr414>

## Original Article

# Histopathological patterns of nephrocalcinosis: a phosphate type can be distinguished from a calcium type

Thorsten Wiech<sup>1,2</sup>, Helmut Hopfer<sup>3</sup>, Ariana Gaspert<sup>4</sup>, Susanne Banyai-Falger<sup>5</sup>, Martin Hausberg<sup>6</sup>, Josef Schröder<sup>7</sup>, Martin Werner<sup>2</sup> and Michael J. Mihatsch<sup>3</sup>

<sup>1</sup>Centre of Chronic Immunodeficiency, University Medical Center Freiburg, University of Freiburg, Freiburg, Germany, <sup>2</sup>Institute of Pathology, University Hospital Freiburg, Freiburg, Germany, <sup>3</sup>Institute for Pathology, University Hospital Basel, Basel, Switzerland, <sup>4</sup>Institute of Surgical Pathology, University Hospital Zurich, Zurich, Switzerland, <sup>5</sup>Klinik St Anna, Luzern, Switzerland, <sup>6</sup>Städtisches Klinikum Karlsruhe, Karlsruhe, Germany and <sup>7</sup>Institute of Pathology, University Hospital Regensburg, Regensburg, Germany

Correspondence and offprint requests to: Thorsten Wiech; E-mail: thorsten.wiech@uniklinik-freiburg.de

## Abstract

**Background.** The etiology of nephrocalcinosis is variable. In this study, we wanted to elucidate whether the histopathological appearance of calcium phosphate deposits provides information about possible etiology.

**Methods.** Autopsy cases from the years 1988 to 2007 and native kidney biopsies from a 50-year period (1959–2008) with nephrocalcinosis were identified. The biopsy cases were re-evaluated by light microscopy. The autopsy cases were analysed according to the underlying disease. The biopsy cases were grouped with respect to the likely etiology of nephrocalcinosis. Total number, density, localization, size and pattern of all calcification foci were documented and correlated with clinical and laboratory data.

**Results.** About 223 of 12 960 autopsy cases (1.7%) had nephrocalcinosis, 111 of which (49.8%) suffered from advanced malignant tumours. Nephrocalcinosis was the main diagnosis in 48 of 12 480 native kidney biopsies (0.4%). Clinicopathological correlation revealed a specific pattern of calcification associated with hyperphosphataemia and/or hyperphosphaturia: these cases showed predominant globular or shell-like calcifications (phosphate type). In contrast, the biopsies of the hypercalcaemic/hypercalciuric group had a different predominant pattern with clumpy or finely granular calcifications (calcium type).

**Conclusions.** Our results indicate that hyperphosphaturia-associated cases of nephrocalcinosis can be distinguished from hypercalciuria-associated cases histopathologically.

**Keywords:** colonoscopy; histopathology; hypercalciuria; hyperphosphaturia; nephrocalcinosis

## Introduction

Nephrocalcinosis is a clinical term defined as the renal deposition of calcium. This definition includes deposits of different chemical composition, such as calcium oxalate or calcium phosphate, and can, but does not have to be

associated with nephrolithiasis. Pathologists distinguish between oxalosis and nephrocalcinosis, the latter again covering different compositions but excluding calcium oxalate. Traditionally, pathologists used the term ‘calcium nephrosis’ for dystrophic calcification i.e. calcification of necrosis and the term ‘nephrocalcinosis’ for metastatic calcification [1]. In our study, we defined nephrocalcinosis as metastatic renal calcifications (excluding oxalosis) by histopathological detection of calcium deposits without associated tissue necrosis.

Nephrocalcinosis can be classified according to the localization of the deposits: calcium can precipitate predominantly in the medulla, as for example in the medullary sponge kidney. Calcifications mainly located in the renal cortex are found, for example, in cortical necrosis. In contrast to ultrasonography or computed tomography, light microscopy can further distinguish whether calcifications are localized in the tubular lumens, tubular epithelium, tubular basement membrane or in interstitial space [2]. On the other hand, nephrocalcinosis can be classified according to the chemical composition, which is likely associated with the etiology of renal calcification. Typically, calcium precipitates with anions in the kidney forming calcium oxalate or calcium phosphate (as hydroxyl apatite) deposits.

Renal calcium deposits occur (i) in disorders associated with impaired homeostasis and an increased renal excretion of calcium or phosphate or (ii) by an altered solubility, e.g. due to a locally altered pH value in the course of renal tubular acidosis, hypocitraturia or tissue necrosis. Apart from that, factors facilitating crystal adhesion to the tubular epithelium seem to be a prerequisite for nephrocalcinosis [3–5]. Hypercalciuria can occur with hypercalcaemia (see Table 1, e.g. in primary hyperparathyroidism, elevated vitamin D<sub>3</sub>, sarcoidosis) or with normal serum calcium levels (idiopathic hypercalciuria). In analogy, hyperphosphaturia can be associated with hyperphosphataemia or with normal or low serum phosphate levels due to impaired reabsorption in the tubules.

**Table 1.** Clinicopathological data of 48 biopsy cases with nephrocalcinosis<sup>a</sup>

	Gender (M/F)	Age (years)	Disease/condition	Calcification type (Ca/P)	Calcification foci (number)	Clumpy (%)	Granular (%)	Globular (%)	Shell- like (%)	Onion skin (%)
Hypercalciuria	M	52	Lung cancer	Ca	10	10.0	60.0	10.0	20.0	0.0
	M	3	Lymphoblastic leukemia	Ca	5	40.0	60.0	0.0	0.0	0.0
	M	25	Sarcoidosis	Ca	15	13.3	66.7	20.0	0.0	0.0
	M	51	Sarcoidosis	Ca	19	15.8	36.8	31.6	10.5	5.3
	M	49	Sarcoidosis	Ca	5	40.0	60.0	0.0	0.0	0.0
	F	65	Hyperparathyroidism	Ca	6	16.7	83.3	0.0	0.0	0.0
	F	34	Hyperparathyroidism	Ca	12	25.0	66.7	8.3	0.0	0.0
	M	43	Paracellin 1 mutation	Ca	5	60.0	40.0	0.0	0.0	0.0
	M	13	Dent's disease	Ca	4	0.0	100.0	0.0	0.0	0.0
Hyperphosphaturia	F	62	Phosphate purgatives	P	11	0.0	0.0	9.1	72.7	18.2
	M	75	Phosphate purgatives	P	27	3.7	14.8	29.6	40.7	11.1
	F	67	Phosphate purgatives	P	3	0.0	0.0	66.7	33.3	0.0
	F	69	Phosphate purgatives	P	29	0.0	0.0	37.9	62.1	0.0
	F	78	Phosphate purgatives	P	18	11.1	11.1	27.8	50.0	0.0
	F	49	Phosphate diabetes	P	9	22.2	11.1	44.4	22.2	0.0
	M	10	Nephrotic syndrome	Ca/P	6	0.0	50.0	50.0	0.0	0.0
	F	2	Nephrotic syndrome	P	23	0.0	26.1	34.8	39.1	0.0
	M	1	Nephrotic syndrome	P	8	12.5	25.0	12.5	50.0	0.0
Unknown cause	F	69	Unknown	Ca	13	0.0	53.8	7.7	23.1	15.4
	M	23	Unknown	P	9	33.3	0.0	22.2	44.4	0.0
	M	46	Unknown	Ca	1	100.0	0.0	0.0	0.0	0.0
	F	42	Unknown	P	3	33.3	0.0	66.7	0.0	0.0
	M		Unknown	Ca	149	73.8	26.2	0.0	0.0	0.0
	F	2	Unknown	Ca	36	61.1	33.3	0.0	2.8	2.8
	M	18	Unknown	Ca	5	80.0	20.0	0.0	0.0	0.0
	M	37	Unknown	P	15	13.3	6.7	13.3	66.7	0.0
	F	44	Unknown	P	11	18.2	27.3	18.2	36.4	0.0
	F	69	Unknown	P	29	6.9	0.0	17.2	75.9	0.0
	F	39	Unknown	P	9	11.1	22.2	0.0	66.7	0.0
	M	29	Unknown	Ca	22	63.6	27.3	4.5	0.0	4.5
	F	50	Unknown	Ca	3	33.3	33.3	33.3	0.0	0.0
	F	30	Unknown	P	9	0.0	44.4	22.2	33.3	0.0
	F	51	Unknown	Ca/P	4	50.0	0.0	0.0	50.0	0.0
	F	61	Unknown	P	21	0.0	23.8	47.6	28.6	0.0
	F	69	Unknown	Ca	10	20.0	50.0	0.0	30.0	0.0
	F	53	Unknown	P	9	22.2	11.1	66.7	0.0	0.0
	F		Unknown	P	8	0.0	25.0	0.0	75.0	0.0
	M		Unknown	P	7	28.6	14.3	0.0	57.1	0.0
	M	40	Unknown	Ca	3	100.0	0.0	0.0	0.0	0.0
	M	9	Unknown	P	33	9.1	33.3	24.2	33.3	0.0
	F	32	Unknown	Ca/P	4	0.0	50.0	50.0	0.0	0.0
	M	62	Unknown	Ca	5	60.0	0.0	40.0	0.0	0.0
	M	42	Unknown	Ca	8	37.5	25.0	0.0	37.5	0.0
	F	66	Unknown	Ca	8	62.5	0.0	0.0	37.5	0.0
	M	78	Unknown	Ca	7	71.4	0.0	28.6	0.0	0.0
	F	69	Unknown	Ca	4	25.0	75.0	0.0	0.0	0.0
	M	36	Unknown	Ca	41	12.2	46.3	17.1	24.4	0.0
	M	73	Unknown	P	11	9.1	0.0	63.6	27.3	0.0

<sup>a</sup>Overview of the findings in all 48 biopsy cases: column 4 shows the classification of the respective cases into 'Ca' (calcium type), if the percentage of clumpy plus finely granular calcifications is >50% and 'P' (phosphate type) and if the percentage of globular plus shell-like calcifications is >50%. Three cases could not be classified (Ca/P) because they showed 50% calcium type and 50% phosphate type patterns. Column 5 shows the total number of calcification foci found in the biopsy. Columns 6–10 show the respective frequency of the five different calcification patterns.

Elevated levels of calcium as well as elevated levels of phosphate can lead to calcium phosphate deposits, which can be visualized histochemically by the von Kossa stain. Hyperphosphataemia can be caused by oral sodium phosphate bowel purgative intake, leading to renal calcium phosphate deposition, also referred to as acute phosphate nephropathy [6–8]. Hyperphosphataemia has also been reported in children suffering from nephrotic syndrome [9].

The aim of this study was (i) to determine the frequency of nephrocalcinosis (excluding oxalosis and

dystrophic calcification of necrosis) in autopsies and renal biopsies and (ii) to elucidate whether the etiology of nephrocalcinosis was associated with a special morphological pattern, including appearance, distribution and density of calcifications. A correlation would indicate that the histological examination of calcification patterns could help to determine the possible mechanism and etiology of nephrocalcinosis in a given case, which is important in biopsy cases if nephrocalcinosis is an incidental finding.

## Materials and methods

### *Patients and specimens*

**Frequency.** The frequency of nephrocalcinosis was determined in autopsy cases of the years 1988–2007 ( $n = 12\,960$ ) and in biopsies of native kidneys of the years 1959–2008 ( $n = 12\,480$ ).

**Morphology.** All biopsies with the leading histopathological diagnosis nephrocalcinosis of the years 1959–2008 were included in this study. All available information, such as age, sex, clinical history, symptoms and laboratory parameters was documented. Histological slides of the undecalcified formalin (4%) fixed, paraffin-embedded biopsies were systematically analysed in haematoxylin and eosin (H&E) and periodic acid Schiff (PAS) stains as well as von Kossa and Alizarin stains for visualization of calcium phosphate depositions. Immunohistochemical staining of Tamm-Horsfall protein (Anti-human Tamm-Horsfall Protein monoclonal antibody clone 10.32; Cedarlane laboratories Ltd, Ontario, Canada. Dilution 1:16000) was performed on paraffin sections of selected cases with sufficient shell-like calcification.

### *Quantitative and semiquantitative evaluation*

Firstly, the biopsy area on the slide (square millimeters) was measured and the proportion of renal cortex and medulla (%) was assessed in order to calculate the respective density of calcifications. The density was defined as the number of calcification foci per square millimeters of the biopsy and calculated by dividing the total number of calcification foci found in the biopsy by the total area of the biopsy measured on the slide (foci per square millimeters). The total number of glomeruli and number of obsolescent glomeruli were determined and the percentage of the total area with tubular atrophy and interstitial fibrosis was estimated. The total number of calcification foci were counted and documented with respect to the following features: localization (cortex, medulla), compartment (tubular lumen, tubular epithelium, tubular basement membrane, interstitium or glomerulus), size (smaller than a tubular cell, as large as a single cell, larger than a cell, larger than a tubular cross section) and structure. The morphological patterns of calcification were analysed in detail. The results were expressed as percent of all calcification foci in the individual biopsy.

### *Energy-filtered electron microscopy*

In order to further characterize the composition of the shell-like calcifications observed in the phosphate type of nephrocalcinosis, energy-filtered electron microscopy was performed. This technique, described in detail elsewhere [10], provides high-resolution imaging with specific element detection and localization [11]. Shell-like calcifications were examined using this method in order to determine the chemical composition, particularly the presence of calcium, phosphorus and oxygen within the optically empty centres.

### *Statistical analysis*

Statistical analysis was done with Prism 5 (GraphPad Software, Inc, La Jolla, CA) using the non-parametric Mann–Whitney test. The morphological and clinical parameters were correlated with each other using Pearson's correlation coefficient.

## Results

### *Frequency*

In 223 of 12 960 (1.7%) autopsy cases from the years 1988 to 2007, nephrocalcinosis was a noteworthy finding. Around 111 of the patients (49.8%) had advanced malignant tumours (Figure 1A), in only two of the others, the etiology could be determined; one patient suffered from sarcoidosis and one from primary hyperparathyroidism.

In 48 of 12 480 native renal biopsy cases (0.4%), nephrocalcinosis was a leading diagnosis (Table 1). In the last of 10 five-year periods (2004–2008), there was an increase in the number of biopsies with nephrocalcinosis (19 cases), compared to the earlier 5-year periods (0–8 cases, Figure 1B). As illustrated in Figure 1B, about half

of the cases showed the calcium type and the other half showed the phosphate type of calcification (see below).

### *Morphology*

Five different patterns of calcifications could be distinguished: clumpy, finely granular, globular, shell-like and onion skin-like (see Figure 2). The overall frequencies (of total 742 calcifications) of the different patterns were 30.1% clumpy, 30.1% finely granular, 15.8% globular, 22.8% shell-like and 1.3% onion skin-like. H&E stain proved to be the best for the differentiation of the calcification patterns. Neither von Kossa stain nor Alizarin stain allowed the differentiation of the different patterns of calcification.

Median age of the patients ( $n = 48$ ) was 44.9 years (1–74.8 years) and half of the patients were females (24 of 48). Mean serum creatinine was 218 (19–800)  $\mu\text{mol/L}$ , mean serum calcium 2.55 (2.0–4.1)  $\text{mmol/L}$  and mean serum phosphate was 1.31 (0.9–3.1)  $\text{mmol/L}$ .

The biopsies contained 0 to 97 (median 15) glomeruli. The percentage of globally obsolescent glomeruli ranged from 0 to 75% (median 11%). Tubular atrophy and interstitial fibrosis varied from 0 to 95% (median 10%). The density of calcification foci ranged from 0.01 to 14.9 foci per square millimeters (average 1.65/ $\text{mm}^2$ ), 0 to 36.7 foci/ $\text{mm}^2$  in the cortex and 0 to 5.6 foci/ $\text{mm}^2$  in the medulla. In 32 biopsies containing renal cortex and medulla, it was possible to evaluate the predominant location of nephrocalcinosis. In 18 of these 32 cases (56%), the calcification density was higher in the medulla and in 14 cases (44%), the density was higher in the cortex. The number of calcification foci adjusted according to the mean biopsy area (15.4/ $\text{mm}^2$ ) was 25.4 foci on average.

Total calcification density did not correlate significantly with serum creatinine levels [correlation coefficient  $r = 0.37$  ( $P = 0.1904$ , 95% CI 0.20–0.75)] nor with calcium  $\times$  phosphate product [ $r = 0.27$  ( $P = 0.28$ , 95% CI 0.23–0.65)]. No significant correlation was found between serum calcium and serum creatinine [ $r = 0.18$  ( $P = 0.3987$ , 95% CI 0.24–0.54)]. However, there was a significant correlation between serum phosphate and serum creatinine [ $r = 0.84$  ( $P = 0.0001$ , 95% CI 0.57–0.94)] and between the calcium  $\times$  phosphate product and serum creatinine [ $r = 0.88$  ( $P < 0.0001$ , 95% CI 0.67–0.96)].

The likely etiology of nephrocalcinosis in our biopsy cases could be identified in 18 of 48 cases: malignant tumours ( $n = 2$ ; one acute lymphoblastic leukemia and one metastatic lung cancer), sarcoidosis ( $n = 3$ ), primary hyperparathyroidism ( $n = 2$ ), paracellin 1 mutation ( $n = 1$ ), Dent's disease ( $n = 1$ ), intake of sodium phosphate bowel purgatives before colonoscopy ( $n = 5$ ), children with nephrotic syndrome ( $n = 3$ ) and phosphate diabetes ( $n = 1$ ). In the remaining cases, the etiology remained unclear even after careful re-evaluation of the clinical records (Table 1).

These 18 cases with known etiology were then divided into two major groups according to the likely mechanism: (i) diseases and conditions associated with hypercalcaemia and/or hypercalciuria (malignant tumours, sarcoidosis, hyperparathyroidism, paracellin 1 mutation, Dent's disease) defined as the 'calcium group' and (ii) diseases and

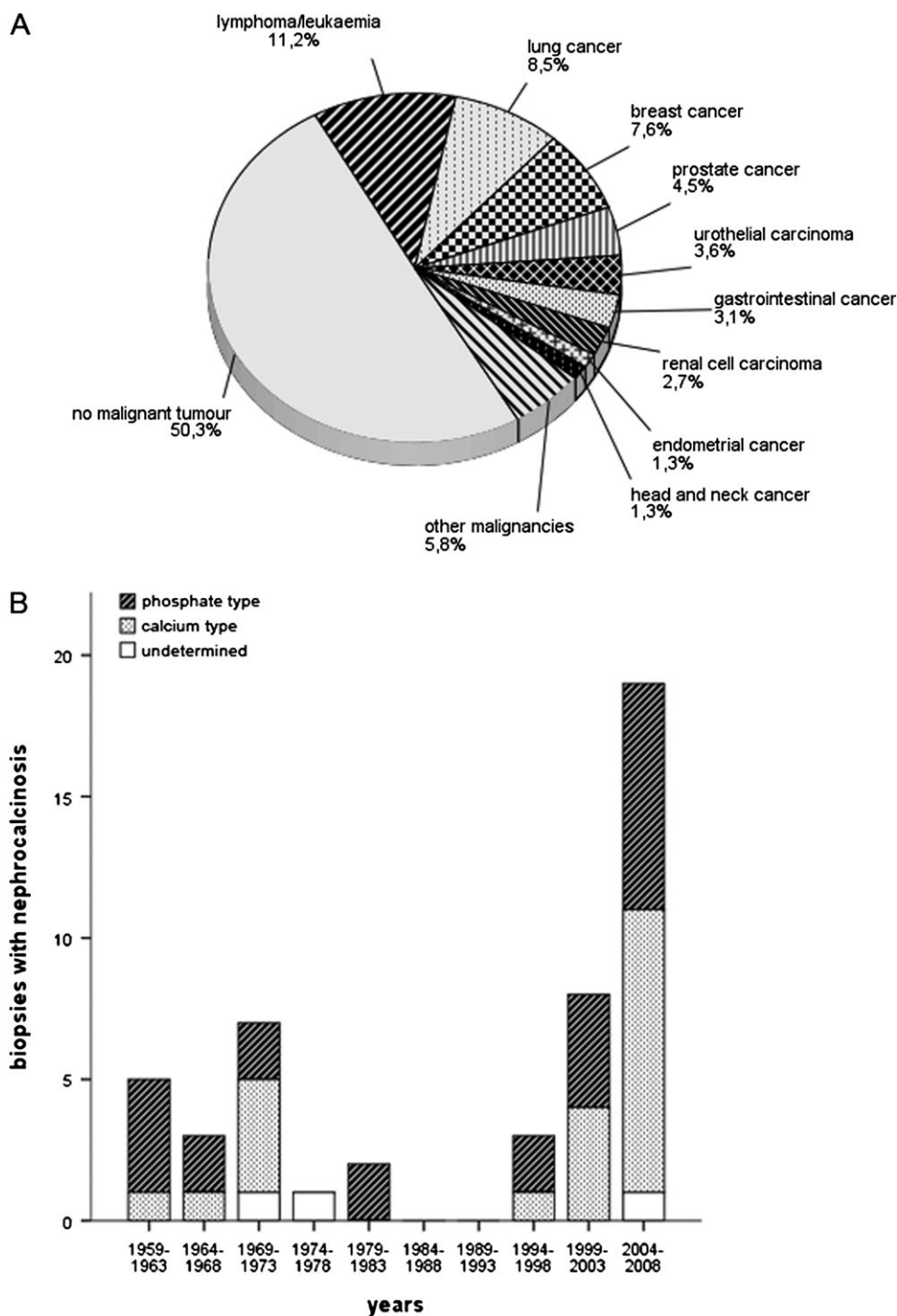


**Fig. 1.** Frequency of nephrocalcinosis. **(A)** Autopsy cases: 111 of 223 (49.7%) cases of nephrocalcinosis were associated with malignant tumours. Twenty-five of them had haematological neoplasia, followed by lung (19 cases) and breast (17 cases) cancer, most of which had bone metastases. **(B)** Frequency of nephrocalcinosis in native kidney biopsies over the years. Note: there was a clear increase in the last 5 years (19 cases in 2004–2008). About half of the cases showed a calcium type and the other half a phosphate type calcification pattern. In three cases, the calcification type could not be assigned to the calcium or phosphate type since half of the calcifications within the respective biopsies showed calcium type patterns and half showed phosphate type patterns.

conditions associated with hyperphosphataemia and/or hyperphosphaturia (sodium phosphate bowel purgatives, nephrotic syndrome in children and phosphate diabetes) defined as the 'phosphate group'. All three children with nephrotic syndrome had normal serum calcium levels and no other reason for nephrocalcinosis could be identified in

the clinical records. Thus, since hyperphosphaturia can occur in children with nephrotic syndrome [9], we classified these cases as members of the phosphate group. In regard to the predominant morphological patterns of the calcium and phosphate group, a striking difference could be observed. In the calcium group, the clumpy and the finely granular



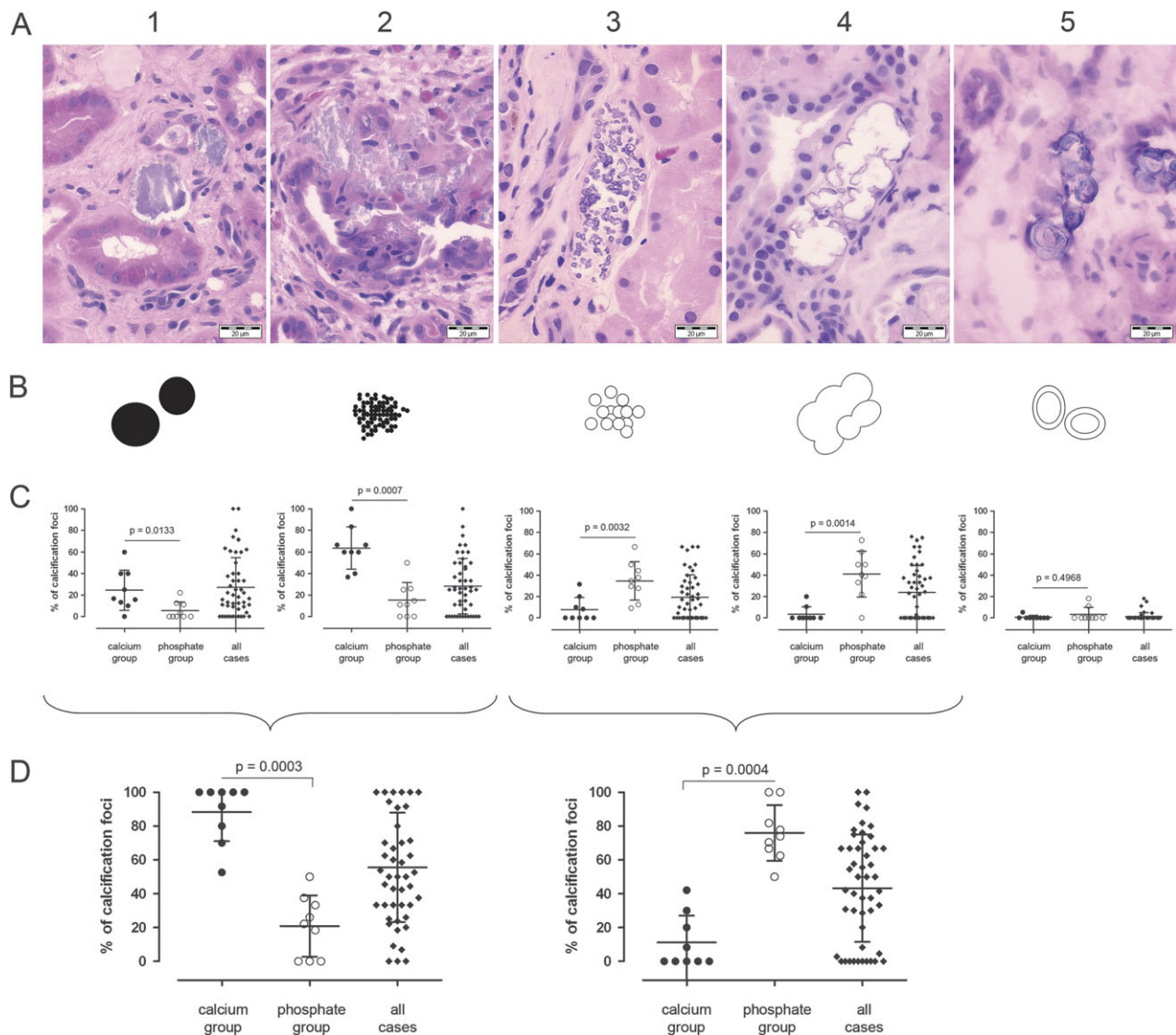


**Fig. 2.** Histopathological patterns of nephrocalcinosis. (A) Five different histopathological patterns (H&E  $\times 400$ , scale bars 20  $\mu\text{m}$ ) and (B) schematic illustration: Column 1, clumpy pattern with homogenous calcifications; column 2, finely granular pattern; column 3, globular pattern with small hollow spherules; column 4, shell-like pattern with thin outer calcifications surrounding empty cores and column 5, onion skin-like pattern with multilayered calcifications. (C) The group of ‘hypercalciuria’ showed predominant calcification patterns 1 and 2 (clumpy and finely granular). In contrast, cases of ‘hyperphosphaturia’ had a predominance of patterns 3 and 4 (globular and shell-like). Only very few onion skin-like calcifications were found. (D) After combining patterns 1 + 2 and 3 + 4, significant differences could be observed: patterns 1 + 2 were associated with conditions leading to hypercalciuria (calcium type) ( $P = 0.0003$ ), whereas patterns 3 + 4 were associated with conditions leading to hyperphosphaturia (phosphate type) ( $P = 0.0004$ ).

patterns predominated. In contrast, in the phosphate group, the most frequent pattern was the shell-like calcification, followed by the globular pattern. Patterns 1–4 reached statistical significance, when the frequencies in the two major disease groups were compared (Figure 2): Patterns 1 and 2 (clumpy and finely granular) were significantly ( $P = 0.0133$  and  $P = 0.0007$ ) more frequent in the calcium group of diseases, whereas Patterns 3 and 4 (globular and shell-like) were significantly ( $P = 0.0032$  and  $P = 0.0014$ ) more frequent in the phosphate group of conditions. The differences of Pattern 5 (onion skin-like) were not statistically significant, this may have been due to its very low overall occurrence rate. Regarding these results, Patterns 1 and 2 were combined and defined as the ‘calcium type’ (1 + 2) and Patterns 3 and 4 as the ‘phosphate type’ (3 + 4) of

nephrocalcinosis. These grouped patterns again showed significant differences between both major groups using the Mann–Whitney test (Figure 2).

In order to assess how specific the phosphate type of calcification was for the intake of sodium phosphate purgatives, we performed a blinded test with a subgroup of 12 cases: PAS-stained slides from four patients with phosphate nephropathy after colonoscopy and eight patients from the other defined classes (tumor, hyperparathyroidism, paracellin 1 mutation, nephrotic syndrome and phosphate diabetes). The blinded set was shown to two experienced nephropathologists (H.H. and M.M.), who were asked to identify the cases of phosphate nephropathy after colonoscopy by using two given criteria: (i) predominance of cortical calcifications and (ii) predominance of

spheroidal or globular intratubular or interstitial clear deposits with shell-like calcifications. In the blinded test for the identification of colonoscopy cases, one of four cases was not classified as a colonoscopy case by one of the two pathologists and one case with nephrotic syndrome was wrongly classified as a colonoscopy case by both pathologists. The overall sensitivity according to the question 'which cases belong to the colonoscopy group?' was 87.5% and the specificity was 77.8%. If the question had been 'which cases belong to the phosphate group?' the sensitivity would have been 90% and the specificity even 100%, because the nephrotic syndrome was also classified as a hyperphosphaturic condition in our study.

In regard to all cases, including those with unknown etiology, we found that 24 cases (50%) of all 48 biopsies with nephrocalcinosis had a predominant calcium type of calcifications. Twenty-one cases (44%) showed a predominance of the phosphate type, although in most of the cases a likely underlying condition leading to nephrocalcinosis could not be determined retrospectively. In three cases (6%), we could not determine the calcification type, since half of the foci were of the calcium and the other half of the phosphate type, respectively (Figure 1B).

In order to further characterize the shell-like calcifications, additional techniques were applied. Von Kossa and Alizarin stain demonstrated the presence of phosphate and calcium within the shell-like calcifications, respectively. Immunohistochemically, Tamm-Horsfall protein could be shown in the shells of the deposits (Figure 3). Energy-filtered electron microscopy revealed calcium, phosphor and oxygen molecules as main components within the shells of the phosphate-type calcifications (Figure 4). In contrast to our assumption that the optically empty centres of these calcifications might predominantly consist of phosphate, we could not detect phosphor and oxygen within the centers but only in the shells.

No clear differences of the localization or sizes of calcification foci were seen between both major groups. In cases of acute phosphate nephropathy after colonoscopy, however, most of the calcifications were intratubular and located in the renal cortex. Apart from the different calcification patterns of hypercalciuria and hyperphosphaturia, cases of sarcoidosis could be distinguished from other subtypes of calcium type nephrocalcinosis by the presence of epithelioid granulomatous reactions, adjacent to the calcifications.

## Discussion

The overall frequency of nephrocalcinosis, defined as renal deposition of calcium-containing molecules (excluding calcium oxalate), observed in autopsies and in native renal biopsies is low (autopsies 1.7%, biopsies 0.4%) but has increased in the last 5 years. One reason could be an increased number of patients receiving sodium phosphate solutions for bowel cleansing before colonoscopy [12]. However, this seems not to be the only cause since not only the phosphate type of nephrocalcinosis, which is typical for phosphate nephropathy, but the calcium type as well has been observed more frequently in the last 5 years.

Malignant tumours were identified in only 2 of 48 cases (4.2%) in our biopsy study. In contrast, in the autopsy study, in 111 (49.8%) cases advanced malignant tumours were found. This discrepancy can be explained by the fact that most of the tumour patients do not undergo renal biopsy because they do not suffer from renal insufficiency or renal insufficiency is not the leading problem that has to be clarified by renal biopsy. The most likely reasons for malignancy-associated nephrocalcinosis are the presence of bone metastases (osteolytic type) or, probably less frequently, production of PTH related peptides (humoral type) by the tumour cells [13].

The main result of our study is the observation that two different major types of renal calcification can be distinguished simply by light microscopy. The two patterns that characterize the calcium type show finely granular or clumpy deposits. This type is associated with malignant tumours, hyperparathyroidism, sarcoidosis, Dent's disease or paracellin-1 mutations. The phosphate type, in contrast, is defined by the presence of shell-like or globular deposits and probably consists of a phosphate rich core, which may be associated with several other molecules, surrounded by a thin layer of calcium phosphate, Tamm-Horsfall protein, and perhaps other substances. However, energy-filtered electron microscopy could only reveal the presence of calcium, phosphor and oxygen in the shells but not within the optically empty centres. Thus, we cannot identify the chemical composition of the cores of these calcifications and we cannot exclude washing out of the material in the centers during the fixation process. This phosphate type in our study is associated with intake of sodium phosphate solutions, nephrotic syndrome in children or phosphate diabetes (Table 2).

The two different patterns likely reflect different mechanisms of crystal formation; the calcium type could be composed predominantly of calcium hydroxyl apatites [14]. In contrast, the shell-like formations of the phosphate type seem to be quite similar to a self-organizing phenomenon forming concentric-lamellated structures called Liesegang rings. This similarity is especially apparent in the electron microscopic appearance of the deposits. The process of Liesegang phenomenon is thought to involve diffusion, nucleation, flocculation or precipitation and supersaturation. Liesegang-like rings have also been described in cysts or in fibrotic, inflamed or necrotic tissue of kidney, synovium, conjunctiva and eyelid [15, 16].

It is well known that nephrocalcinosis also occurs in renal allografts. Likely reasons are hyperparathyroidism [17], drug toxicity, as described for calcineurin inhibitors [18, 19] and hyperphosphaturia due to denervation [20]. Our observation can also be applied to nephrocalcinosis in renal allograft biopsies to distinguish hyperphosphaturic from hypercalciuric forms. The phosphate type could be associated with calcineurin inhibitors since for example, FK506 (tacrolimus) can lead to increased excretion of phosphate [21], whereas the calcium type could rather be associated with hyperparathyroidism (Table 2). However, whether this is really true and helpful to determine the likely cause has to be elucidated in further studies. Early nephrocalcinosis in the renal allograft is sometimes associated with hyperparathyroidism and is correlated with



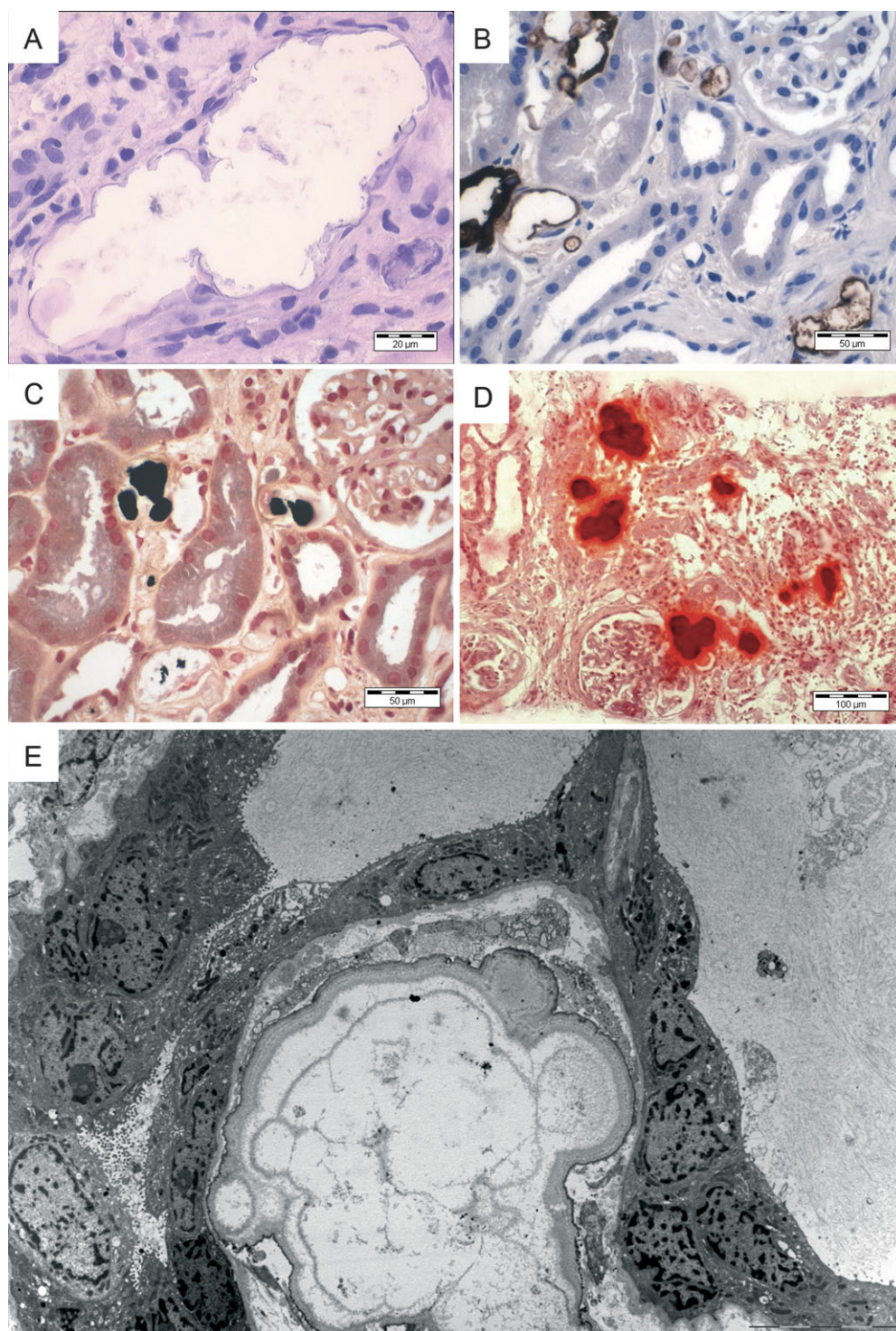


**Fig. 3.** Characteristics of the shell-like calcifications in the phosphate type of nephrocalcinosis after intake of sodium phosphate bowel purgatives before colonoscopy: (A) Shell-like calcifications (H&E,  $\times 400$ , scale bar 20  $\mu\text{m}$ ). (B) Immunohistochemical staining for Tamm-Horsfall protein shows positivity in the shells of the calcification foci ( $\times 200$ , scale bar 50  $\mu\text{m}$ ). (C) Von Kossa reaction visualizes deposition of anions (phosphate) ( $\times 200$ , scale bar 50  $\mu\text{m}$ ) and (D) Alizarin reaction shows calcium depositions within the calcification foci ( $\times 100$ , scale bar 100  $\mu\text{m}$ ). (E) Electron microscopy reveals a lamellated structure of the calcifications with a very thin outer electron dense layer and some lighter concentric inner layers ( $\times 1400$ , scale bar 10  $\mu\text{m}$ ).

inferior outcome compared to renal allografts without calcifications [22]. However, in paediatric patients, renal allograft calcification seems to be neither correlated with hypercalciuria nor with a negative influence on graft function [23].

Calcifications in patients who received sodium phosphate solutions seemed to be localized predominantly in the renal cortex. In some patients with other causes of nephrocalcinosis, including calcium types, there was, however, also predominant cortical calcification and, moreover,



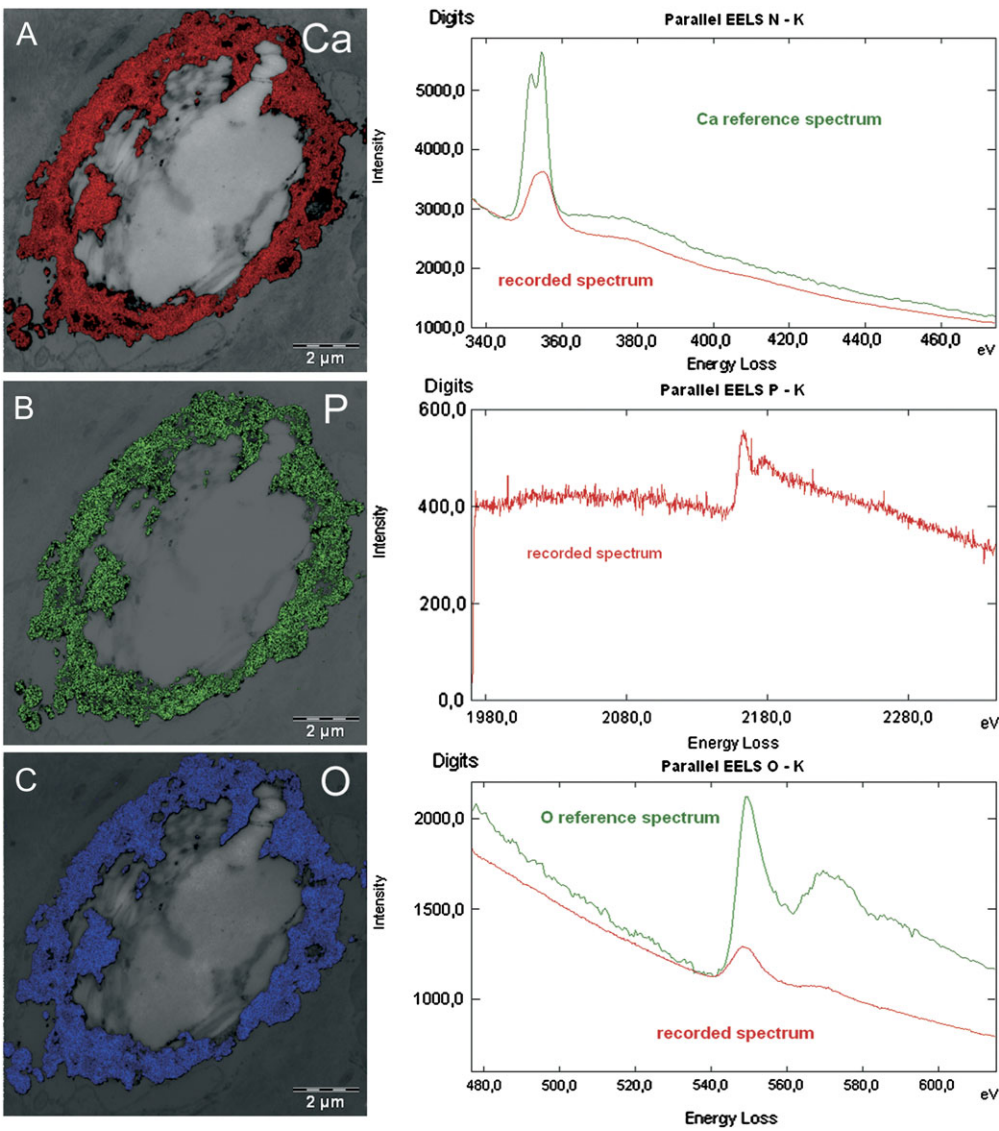


**Fig. 4.** Energy-filtered electron microscopy of a case with shell-like and globular calcifications of the phosphate type demonstrates the presence of (A) calcium, (B) phosphor and (C) oxygen molecules within the shells of calcifications with the respective energy loss spectrum on the right.

**Table 2.** Proposed classification of nephrocalcinosis into calcium and phosphate types<sup>a</sup>

Calcium type (associated with hypercalciuria)	Phosphate type (associated with hyperphosphaturia)
With hyperphosphataemia Tumor (osteolytic or humoral type) Hyperparathyroidism Sarcoidosis and other granulomatous diseases Vitamin D excess Infantile hypercalcaemia	With hyperphosphataemia Sodium phosphate purgatives Children with nephrotic syndrome
Without hypercalcaemia Idiopathic hypercalciuria Dent's disease Renal allografts Hyperparathyroidism	Without hyperphosphataemia Phosphate diabetes  Renal allografts Calcineurin inhibitor toxicity

<sup>a</sup>Conditions and diseases likely associated with hypercalciuria (with or without hypercalcemia) and hyperphosphaturia (with or without hyperphosphatemia) classified according to the expected type of calcification (calcium type with finely granular or clumpy calcifications and phosphate type with globular or shell-like calcifications).

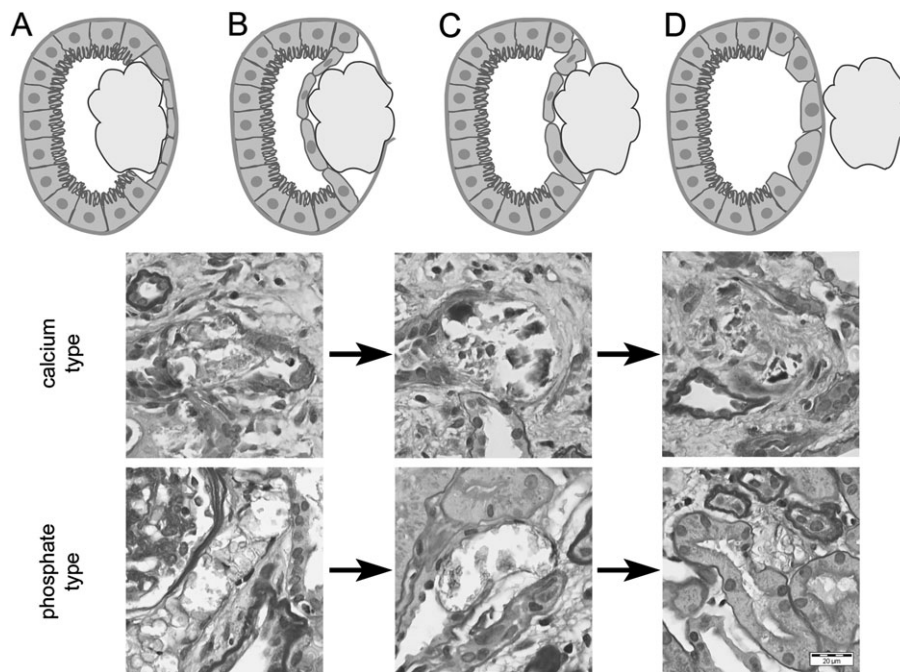


**Fig. 5.** Hypothetical mechanism of migration of larger intratubular calcifications illustrated schematically (first row) and with examples of calcium type (second row) and phosphate type (third row) calcifications (PAS stain,  $\times 400$ ): Initially, the intratubular deposit destroys tubular epithelial cells (**A**) and leads to 'defects' of the tubular basement membrane (**B**). Regenerated tubular epithelial cells cover the calcification and the deposit migrates (**C**) out of the tubule until it is finally located in the interstitial space. Mostly, the tubular basement membrane shows no thickening or multilayering.

some biopsies did not contain tissue of the renal medulla. Thus, the distribution of the calcifications concerning cortex or medulla in our study did not provide much information about the possible cause.

Many of the calcifications seen in phosphate nephropathy were localized within the tubular lumens. In contrast, some of the calcium types of nephrocalcinosis had predominant interstitial calcifications. In our opinion, this could rather reflect a time course, in which the initial phase shows predominant intratubular calcifications and the later stages have predominant interstitial calcifications. This probably reflects a mechanism whereby larger calcium deposits destroy individual tubular cells and then move through the basement membranes into the interstitial space, which subsequently could cause interstitial fibrosis (Figure 5). Since we do not know when precipitation of calcium phosphate started in our cases, we cannot prove the hypothesis in this study. However, the phenomenon of migration of the calcifications from the tubular lumens after epithelial overgrowth into the interstitium or the so-called 'exotubulosis' was recently reported in animal experiments [24]. They also depicted the morphological phenomena outlined in Figure 5 in human renal biopsies. Furthermore, smaller intratubular calcifications, which do not affect the tubular epithelium, are most likely voided in the urine.

In conclusion, simple light microscopy can distinguish a calcium from a phosphate type of nephrocalcinosis, each being associated with different diseases or conditions leading to calcification. Thus, histomorphology of nephrocalcinosis can help the clinician to assess the likely cause of renal calcification.

**Acknowledgements.** We thank Ursula Dürmüller and Claudia Lautenschlager for excellent technical assistance, Prof. Dr Stephen Batsford for the critical review of the manuscript and all nephrologists, who provided information about the patients.

**Conflict of interest statement.** None declared.

## References

1. Zollinger HU. Die Nephrocalcinose und die Kalknephrose. In: Zollinger HU ed *Niere und ableitende Harnwege*. Berlin, Germany: Springer-Verlag; 1966
2. Verkoelen CF, Verhulst A. Proposed mechanisms in renal tubular crystal retention. *Kidney Int* 2007; 72: 13–18
3. Lieske JC, Deganello S. Nucleation, adhesion, and internalization of calcium-containing urinary crystals by renal cells. *J Am Soc Nephrol* 1999; 10 (Suppl 14): 422–429
4. Vervaeke BA, D'Haese PC, De Broe ME *et al*. Crystalluric and tubular epithelial parameters during the onset of intratubular nephrocalcinosis: illustration of the 'fixed particle' theory in vivo. *Nephrol Dial Transplant* 2009; 24: 3659–3668
5. Vervaeke BA, Verhulst A, De Broe ME *et al*. The tubular epithelium in the initiation and course of intratubular nephrocalcinosis. *Urol Res* 2010; 38: 249–256
6. Martin RR, Lisehora GR, Braxton M Jr *et al*. Fatal poisoning from sodium phosphate enema. Case report and experimental study. *JAMA* 1987; 257: 2190–2192
7. Markowitz GS, Nasr SH, Klein P *et al*. Renal failure due to acute nephrocalcinosis following oral sodium phosphate bowel cleansing. *Hum Pathol* 2004; 35: 675–684
8. Desmeules S, Bergeron MJ, Isenring P. Acute phosphate nephropathy and renal failure. *N Engl J Med* 2003; 349: 1006–1007
9. Feinstein S, Becker-Cohen R, Rinat C *et al*. Hyperphosphatemia is prevalent among children with nephrotic syndrome and normal renal function. *Pediatr Nephrol* 2006; 21: 1406–1412

10. Schroeder JA, Weingart C, Coras B *et al.* Ultrastructural evidence of dermal gadolinium deposits in a patient with nephrogenic systemic fibrosis and end-stage renal disease. *Clin J Am Soc Nephrol* 2008; 3: 968–975
11. Keast VJ, Bosman M. New developments in electron energy loss spectroscopy. *Microsc Res Tech* 2007; 70: 211–219
12. Markowitz GS, Stokes MB, Radhakrishnan J *et al.* Acute phosphate nephropathy following oral sodium phosphate bowel purgative: an underrecognized cause of chronic renal failure. *J Am Soc Nephrol* 2005; 16: 3389–3396
13. Weiss M, Liapis H, Tomaszewski JE *et al.* Pyelonephritis and other infections, reflux nephropathy, hydronephrosis, and nephrolithiasis. In: Jennette JC, Olson JL, Schwartz MM, Silva FG (eds) *Heptinstall's Pathology of the Kidney*. Philadelphia, PA: Lippincott Williams & Wilkins; 2006
14. Zollinger HU, Mihatsch MJ. Nephrocalcinosis. In: *Renal Pathology in Biopsy*. Berlin, Germany: Springer Verlag, 1978, pp. 483–486
15. Tuur SM, Nelson AM, Gibson DW *et al.* Liesegang rings in tissue. How to distinguish Liesegang rings from the giant kidney worm, *Diectophyma renale*. *Am J Surg Pathol* 1987; 11: 598–605
16. Sniege N, Dekmezian R, Zaatari GS. Liesegang-like rings in fine needle aspirates of renal/perirenal hemorrhagic cysts. *Acta Cytol* 1988; 32: 547–551
17. Schwarz A, Mengel M, Gwinner W *et al.* Risk factors for chronic allograft nephropathy after renal transplantation: a protocol biopsy study. *Kidney Int* 2005; 67: 341–348
18. Marbet UA, Graf U. Renale Nebenwirkungen der Therapie mit Cyclosporin A bei chronischer Polyarthrit und nach Knochenmarkstransplantation. *Schweiz Med Wochenschr* 1980; 110: 2017
19. Mihatsch MJ, Gudat F, Ryffel B, Thiel G. Cyclosporine nephropathy. In: Tisher TC, Brenner BM (eds) *Renal Pathology*. Philadelphia, PA: Lippincott; 1994, pp. 1641–1681
20. Straub B, Muller M, Heicappell R *et al.* Hyperphosphaturia after kidney transplantation in syngeneic rats: effects on nephrocalcinosis and bone metabolism? *Transplant Proc* 2003; 35: 1575–1580
21. Mohebbi N, Mihailova M, Wagner CA. The calcineurin inhibitor FK506 (tacrolimus) is associated with transient metabolic acidosis and altered expression of renal acid-base transport proteins. *Am J Physiol Renal Physiol* 2009; 297: 499–509
22. Gwinner W, Suppa S, Mengel M *et al.* Early calcification of renal allografts detected by protocol biopsies: causes and clinical implications. *Am J Transplant* 2005; 5: 1934–1941
23. Habbig S, Beck BB, Feldkotter M *et al.* Renal allograft calcification—prevalence and etiology in pediatric patients. *Am J Nephrol* 2009; 30: 194–200
24. Vervaeke BA, Verhulst A, Dauwe SE *et al.* An active renal crystal clearance mechanism in rat and man. *Kidney Int* 2009; 75: 41–51

Received for publication: 30.11.10; Accepted in revised form: 17.6.11